ACS APPLIED MATERIALS & INTERFACES

Research Article

www.acsami.org

Photoresponse of a Single Y-Junction Carbon Nanotube

Sudeshna Samanta,*[,†,⊥] Deepika Saini,[‡] Achintya Singha,[§] Kaustuv Das,[†] Prabhakar R. Bandaru,[∥] Apparao M. Rao,[‡] and Arup Kumar Raychaudhuri*[,†]

[†]Unit for Nanosciences, Department of Condensed Matter Physics and Material Sciences, S. N. Bose National Centre for Basic Sciences, Salt Lake, Kolkata, West Bengal 700091, India

[‡]Department of Physics and Astronomy and Clemson Nanomaterials Centre, Clemson University, Clemson, South Carolina 29634, United States

[§]Bose Institute, 93/1, Acharya Prafulla Chandra Road, Kolkata, West Bengal 700009, India

[∥]Department of Mechanical and Aerospace Engineering, University of California, San Diego, La Jolla, California 92093, United States

Supporting Information

ABSTRACT: We report investigation of optical response in a single strand of a branched carbon nanotube (CNT), a Y-junction CNT composed of multiwalled CNTs. The experiment was performed by connecting a pair of branches while grounding the remaining one. Of the three branch combinations, only one combination is optically active which also shows a nonlinear semiconductor-like *I*−*V* curve, while the other two branch combinations are optically inactive and show linear ohmic *I*−*V* curves. The photoresponse includes a zero-bias photocurrent from the active branch combination. Responsivity of ≈1.6 mA/W has been observed from a single Y-CNT at a moderate bias of 150 mV with an illumination of wavelength 488 nm. The photoresponse experiment allows us to understand the nature of internal connections in the Y-CNT. Analysis of data locates the region of photoactivity at the junction of only two branches and only the combination of these two branches (and not individual branches) exhibits photoresponse upon illumination. A model calculation based on back-to-back Schottky-type junctions at the branch connection explains the *I*−*V* data in the dark and shows that under illumination the barriers at the contacts become lowered due to the presence of photogenerated carriers.

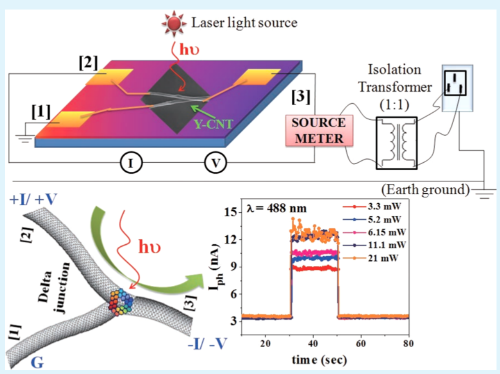

KEYWORDS: *single carbon nanotube, Y-junction, photoresponse, zero-bias photocurrent, low-temperature electrical transport, Schottky barrier*

INTRODUCTION

Single-walled (SW) and multiwalled (MW) carbon nanotubes (CNTs) have been at the center stage of research and development in nanoscale electronic and optoelectronic devices since the discovery of CNTs in 1991.[1] A number of CNT-based nanostructures have been discovered or proposed for nanoelectronics applications.[2,3] The capability to use nanolithography tools to connect electrical leads to a single CNT has added new dimensions to the investigations as it allows electrical and optoelectronic investigations on a single CNT.[3,4]

Other than the straight tubular CNTs, different geometrical shapes like nanotubes with kinks, loops, and multiterminal junctions have been studied. Branched nanotubes with three arms, referred to as a Y-junction CNT (or Y-CNT), have been synthesized and their structure and electrical transport properties have been widely investigated.[5−7] It appears that in a Y-CNT, which involves the use of metal catalysts (e.g., Ni and Ti), the junction has a structure that is different from the bulk. It has been established by transmission electron microscopy (TEM) that the Y-CNT made from MWCNT has a fish-bone structure at the junction region where the graphitic layers that make the nanotubes are oriented at an angle to the axis.[8] The Y-CNT junction regions made from single-wall nanotubes (SWNT) have been suggested to contain topological defects in the form of pentagon and heptagons for maintaining low-energy sp^2 configuration which are necessary to give it the curvature.[9] The fish-bone structure of topological defects at the junction regions can act as scattering centers of electrons that can affect the transport through the junction region. Electrical transport measurements done on single Y-CNT[6] as well as scanning tunneling spectroscopy (STS) studies[8] demonstrate that while one can have symmetric dI/dV in the branches, near the junction the dI/dV curve becomes asymmetric due to emergence of semiconducting behavior. Three terminal Y-CNTs with their self-contained gate terminal have gained enormous interest by providing rectifying properties,[10] switch-

Received: April 9, 2016
Accepted: July 5, 2016
Published: July 5, 2016

DOI: 10.1021/acsami.6b04231
ACS Appl. Mater. Interfaces 2016, 8, 19024−19030

ing,[7] and logic gates.[7] In this paper we establish that the junction region also acts as a center of photovoltaic activity.

Among the various exciting physical properties of CNT-based nanostructures, optical responses have received a great deal of attention due to the nature of exciton photo physics[11] and efficient electron−hole pair generation.[12] A number of investigations addressed the issue of photocurrent in a single CNT, in particular, those that performed spatially resolved scanning photocurrent measurements that can identify the role of localized p−n junctions/Schottky-type barriers in photoresponse.[13−16] Different mechanisms proposed for photoresponse in such systems are intraband transitions and generation of photon-induced excitons, or from Schottky barrier (metal−semiconductor) height modulation. There are also theoretical calculations/models that attempt to explain the photoresponse properties in CNTs.[17−20] In a recent publication, the interest in the optical properties of CNTs has been revived which identifies the differences in the photoresponse in metallic and in semiconducting CNTs.[21] In the former type the response is thermal in origin and is related to the generation of photoexcited hot carriers. In this context it will be interesting to investigate what happens to the photoresponse in a branched CNT nanostructure like a Y-CNT.

In this paper we report photoconductivity in a single Y-CNT that has branches of MWCNTs. It is noted that although electrical transport in single Y-CNT has been studied (as stated before) there is no report of optical responses from Y-CNT. By checking optical response from a combination of branches (arms), we find that the response as detected does not arise from the arms of the Y-CNT but likely from the junction. Interestingly, the Y-CNT junction gives rise to a zero-bias photoresponse, suggesting a photovoltaic-type mechanism for photocurrent generation that would be expected for the semiconducting nature of the junction region. The observed photocurrent increases with applied bias and can reach a value in excess of 400 nA at a small bias of 150 mV for a moderate optical power (at 488 nm) that corresponds to a responsivity of 1.6 mA/W. At zero bias under similar illumination the photocurrent is ≈14 nA and a current gain over a dark current of ≈1.5 or more. The photoresponse experiment, as we will show, gives us an important tool that allows us to understand the connectivity in a Y-CNT.

EXPERIMENTAL SECTION

The Y-CNT junctions were grown on bare quartz or Si/SiO_2 substrates through thermal chemical vapor deposition (CVD). The detailed process has been described elsewhere.[7] Branching in such CNTs occurs due to the presence of topological defects (as stated before) which can be formed by insertion of metal catalyst particle at the junction during synthesis. In our case, the Ti precursor has been used for the junction formation.[7] Figure 1a shows the scanning electron microscopy (SEM) image at low scanning voltage of 5 kV. The average diameter of each branch is 60 nm and the length of each branch (including stem) is ≈5 μm. For electrical and photoresponse studies Y-CNTs were dispersed on a silicon nitride membrane. Contacts to a single Y-CNT were made using Pt deposited by a focused ion beam (FIB) in a dual beam system (Helios 600). The Y-CNT with Pt contact leads is shown in Figure 1b. Any damage due to ion-beam radiation had been avoided, which reduces the defect density inside the tube. The Pt contacts serve as interconnects to Au contact pads which were securely printed on a chip carrier.

The transport properties like temperature (T)-dependent resistivity (ρ) and current−voltage (I−V) characteristics were done by a direct current method. We have taken special care for grounding of the branches for successive measurements among interbranches and intrabranches.[7] This is needed because if the third branch is kept open, it acts as a source of noise. To avoid shorting with a grounded branch, we used a floating source for bias. To achieve floating source, we used an isolation transformer's output connected to our measuring unit's (high-precession digital multimeter) power supply. This arrangement makes the whole system (measuring unit connected to first and second branches) isolated from the Earth's ground. As a result, the third branch becomes automatically disabled to be getting shorted. Additional electromagnetic shielding and use of coaxial cables were used to reduce external noises. We also carried out our experiments with the possible combination of branches as tabulated in Table 1 and from which we identified the linear (photoinactive) and nonlinear (photoactive) branch combinations.

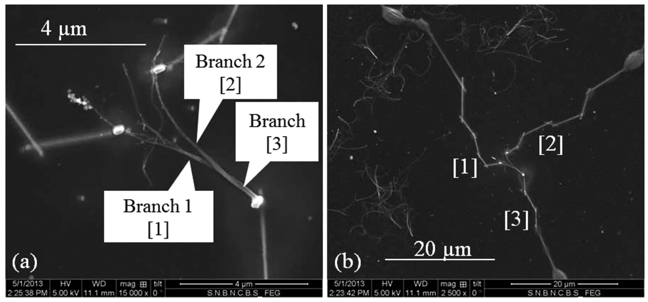

Figure 1. (a) SEM image of a single Y-CNT with two branches and a stem of average diameter 60 nm. (b) The FIB-deposited Pt contact leads are connected with a Y-CNT to form a device.

Table 1. Inter- and Intrabranch Configuration for Study of *I*−*V* Characteristics and Photoresponse

combination of branches	branch grounded	*I*−*V* characteristics		photoresponse
[1]−[2] and [2]−[1]	[3]	linear	ohmic	inactive
[1]−[3] and [3]−[1]	[2]	linear	ohmic	inactive
[2]−[3] and [3]−[2]	[1]	**nonlinear**	**nonohmic**	**active**

RESULTS AND DISCUSSION

Electrical Measurements in the Dark. We measured I−V characteristics at 300 K for all the branch combinations in the dark. The I−V data for all possible combinations like [1]−[2], [1]−[3], and [2]−[3] are shown in Figure 2a−c, respectively. The I−V data shown as (I_{12}−V_{12}) is linear and nearly symmetric. Similar linear I−V data are seen for the branch combination [1]−[3] also. The two branch combinations taken together involve all the three branches as well as two branch contacts. The linearity of the I−V suggests that the three branches and the contacts 13 and 12 are ohmic metallic contacts. Since the branches are made from MWCNTs, observation of the metallic behavior is not unexpected.[6] Interestingly, however, the I−V characteristics for the branch combination [2]−[3] show asymmetric nonlinear behavior as shown in Figure 2c. The branch combinations like [1]−[2] and [1]−[3] are less resistive (ohmic) compared to the particular branch combination [2]−[3] (nonohmic), which can be readily seen by comparing two I−V characteristics. The input voltage V_{23} is nearly 25 times higher than V_{13} to draw the same amount of current. We have restricted our measurement for current ≤800 nA to avoid damage of Y-CNT. The linearity of the I−V data for branch combinations [1]−[2] and [1]−[3] along with

DOI: 10.1021/acsami.6b04231
ACS Appl. Mater. Interfaces 2016, 8, 19024−19030

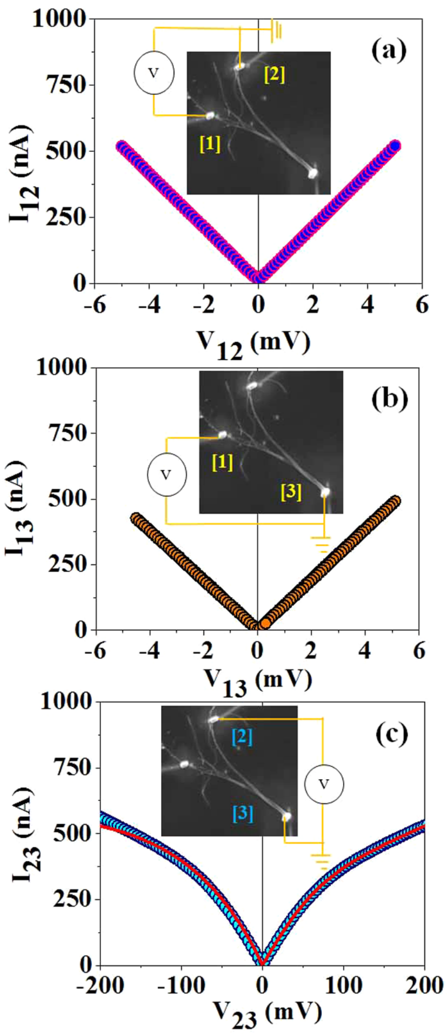

Figure 2. (a, b) Linear and (c) nonlinear $I-V$ characteristic for [1]–[2], [1]–[3], and [2]–[3], respectively, at 300 K. Insets of (a), (b), and (c) show the electrical connections between different branch combinations. The solid lines in Figure 2c show the theoretical fit (eq 1) based on the proposed model of back-to-back Schottky junctions (see text).

the fact that this is nonlinear for the combination [2]–[3] suggest that the contact 23 (between branch [2] and [3]) is nonohmic and has finite barrier to transport. Since branches [2] and [3] show linear behavior, the source of nonlinearity is at the junction region.

The temperature-dependent resistivity data for a Y-CNT are shown in Figure S1 in the Supporting Information. We have measured resistivity (ρ) as a function of temperature (T) with a current of 400 nA between branches [1]–[3]. Similar data are also shown for the branch combination [1]–[2]. The measured resistance as well as calculated $\rho \sim 0.01\Omega$-m at 30 K matches with earlier experiments carried on a single MWCNT.[7,14,22] It is difficult to measure contact resistance exactly in a three terminal device. However, comparing the resistivity value with earlier experimental values confirms low contact resistance and the intrinsic nature of the CNT.[14,22] For the branch combination [2]–[3], the $I-V$ curve being nonlinear (shown in Figure 2c), the resistivity is measured at lower current ($I \leq$ 100 nA). The measured ρ at 30 K is $\approx$10 Ω-m.

Measurement of Photoresponse. Photoresponse has been measured with different branch combinations with two different laser wavelengths λ_1 = 488 nm and λ_2 = 785 nm. Experiments were performed under a laser spot size of 1 μm. Figure 3a shows a schematic diagram of the circuit for photoresponse studies under different light illumination. The data on photoactivity is summarized in Table 1. It has been found that for linear branch combinations [1]–[2] and [1]–[3] there is no photoresponse within detectable current limit (few picoampere). However, in the branch combination [2]–[3], we observed nonlinear and nonohmic behavior. Absence of photoresponse in the other two branch combinations [1]–[2] and [1]–[3] show that none of the branches, which are metallic, show any photoresponse. Similarly, contacts 13 and 12 also cannot be the origin of photoresponse. By elimination of different combinations and the fact that the photoresponse occurs only with the branch combination [2]–[3], it is possible to locate the origin of the photoresponse at the branch contact point 23.

In Figure 3b we show the response of the Y-CNT when the light is switched ON and OFF. The data have been taken with a small bias of ~1.0 mV. The photocurrent (I_{ph}) responds to the power ON/OFF (the speed of light modulation is around a few milliseconds) and there is no persistent photoconductivity observed on power OFF as is seen in photoconductors that have deep trap states. Similar data can also be seen at longer illuminating wavelength λ_2 = 785 nm.

In Figure 3c we show the zero-bias photocurrent ($I_{ph}(V = 0)$) as a function of illumination power. It is noted that the zero-bias current in the dark (arising mainly due to bias current of the amplifier) is ~1.5 nA. Thus, even for the lowest power used the zero-bias photocurrent is larger than the dark current at zero bias. The important aspect of the photoresponse seen with branch combination [2]–[3] is that a finite photocurrent is also seen when no bias is applied between the contacts. The $I_{ph}(V = 0)$ at zero bias has been measured with varying illuminating powers (λ_1 = 488 nm) as shown in Figure 3c. At low illumination, $I_{ph}(V = 0)$ varies linearly with illumination power but it saturates at higher power. Such a saturation of the zero-bias photocurrent may arise due to trapping, and recombination of the carriers within the nanotube, in particular, due to existence of localized traps.[23]

The zero-bias photocurrent has photovoltaic origin where the carrier separation arises due to the built-in potential at the branch contact.[23] We will discuss this issue later on where we propose a simple model of the junction that can give rise to selective photoresponse in a branch contact. It has been observed in different types of nanowires that range from Si nanowires[24] to charge-transfer complex nanowires,[25] and very recently, in networks of Si and Ge nanowires.[26]

In Figure 4a,b we have plotted $I-V$ characteristics measured under illumination for different laser powers available for λ_1 and λ_2. We have restricted our current limit to ~800 nA to avoid the damage of the branch. The Y-axis, I_{ph}, denotes the total current, that is, the sum of dark current I_0 and the photogenerated current from the Y-CNT under illumination. In Figure 4c we have magnified the low-voltage biased region (-6 mV $\leq V \leq$ 6 mV) to record dark current for λ_1 and λ_2, respectively.

In Figure 4d we plotted the gain of the current I_{ph} to the dark current (I_{ph}/I_0) as a function of illumination power for the two illumination wavelengths λ_1, and λ_2 measured with a low applied bias of 50 mV. For both wavelengths, the current gain

DOI: 10.1021/acsami.6b04231
ACS Appl. Mater. Interfaces 2016, 8, 19024–19030

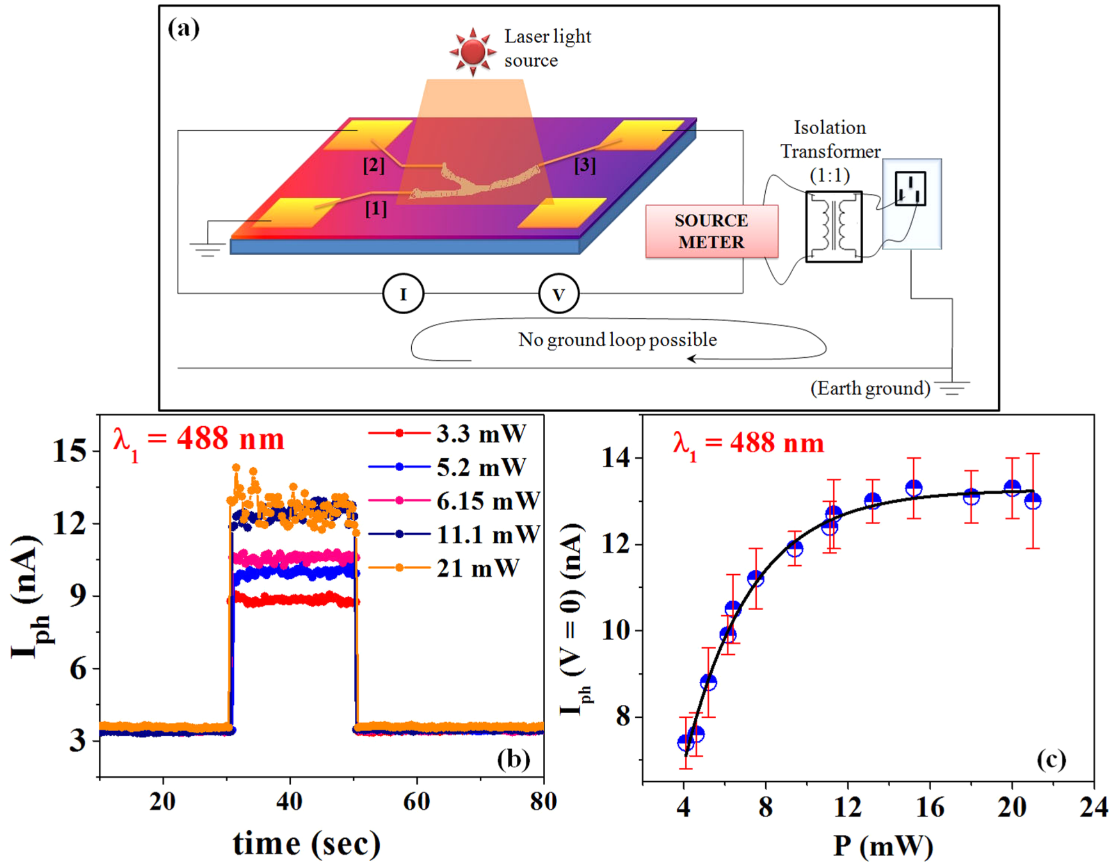

Figure 3. (a) Schematic model of the specific contact behaviors for single Y-CNT and electrical contact pads. (b) The photocurrent (I_{ph}) responds to the power ON/OFF with speed of light illumination. Data were taken with a small applied bias ~1 mV. (c) The power dependence of zero-bias I_{ph} (V = 0) for λ_1.

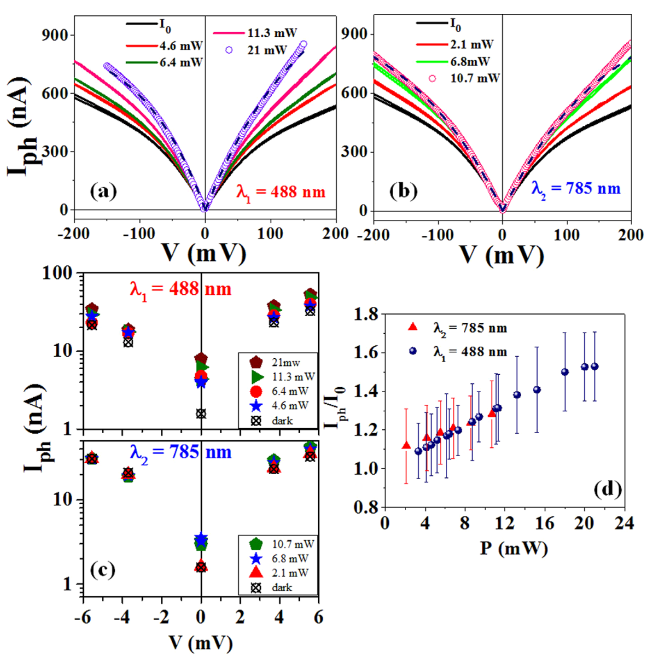

Figure 4. (a, b) I–V characteristics of Y-CNT measured under illumination for different powers available for λ_1 and λ_2, respectively. (c) Magnified I–V curves within −6 mV ≤ V ≤ 6 mV to show the current response at very low bias voltages. (d) Power variation of current gain I_{ph}/I_0 under illumination.

I_{ph}/I_0 is similar and increases linearly with laser power until it saturates as the power →20 mW. This implies broad spectral response. (Note: At zero bias, the photocurrent tends to saturate at a lower laser power, see Figure 4c). Due to limited power availability for the illumination at λ_2, saturation of the photocurrent could not be observed. The observed current gain reaches a value of ≃1.53 for 22 mW of laser power which is much higher than that observed in earlier work on MWCNT bundle ($I_{ph}/I_0 \approx 1.16$ at a similar laser power 24 mW).[14] In the present investigation the photoresponse appears to be originating at the branch junction (23) and not on the branches. The larger current gain would imply that the junction has a higher photoresponse.

We have calculated parameters like responsivity $\mathfrak{R}$ and quantum efficiency Q_e related to conversion efficiency of power of the Y-CNT as tabulated in Table 2 for three representative biases.[14] The values are for the largest power used (21 mW), assuming that all the power that falls over the lengths of the three branches is absorbed. Since this assumption overestimates the power absorbed, the value of $\mathfrak{R}$ (current per unit power

Table 2. Responsivity ($\mathfrak{R}$) and Quantum Efficiency (Q_e) for Photoactive Branch with λ_1 = 488 nm and Power (21 mW)

bias voltage (mV)	ΔI ($\times 10^{-9}$ A)	$\mathfrak{R}$ (mA W^{-1})	Q_e (%)
50	122.3 ± 3.5	0.48 ± 0.01	0.123 ± 0.002
100	247.5 ± 8.5	0.98 ± 0.03	0.249 ± 0.007
150	410.0 ± 11.5	1.63 ± 0.05	0.413 ± 0.012

DOI: 10.1021/acsami.6b04231
ACS Appl. Mater. Interfaces 2016, 8, 19024−19030

absorbed) is an underestimation. (Note: Q_e is defined as $100\times\mathfrak{R}\times(1.2395/\lambda)$). $\mathfrak{R}$ and Q_e both increase with applied bias and the photoresponse of the Y-CNT has a responsivity comparable to that observed in a bundle of SWCNT.[14]

The principal observation is that Y-CNT shows substantial photoresponse, a phenomenon that has not been reported before. It has also been observed that of the three branch combinations only one branch combination that shows nonlinear nonohmic transport ($I-V$) curves show photoresponse. This leads to localization of the photoresponse at a specific branch contact. This also would imply a specific internal structure of connectivity of the branches. This is elaborated upon in Figure 5. When three branches meet, the

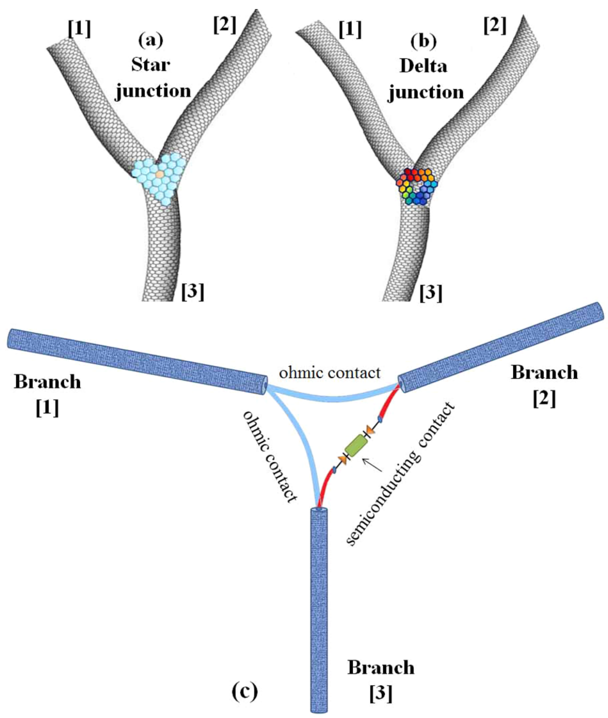

Figure 5. Schematic diagram of the configurations for branch combinations: (a) Star connection and (b) delta connection. (c) Model of the proposed structure of Y-CNT containing a back-to-back Schottky junction along with the branches.

connectivity can have a single point of connection like a "Star" connection as shown in Figure 5a, or it can have distinct pairwise connections of the junctions like a "Delta" connection as shown in Figure 5b. If the transport is measured pairwise, then for the "Star" connection, if one measures two pair combinations like [1]−[2] and [1]−[3], then the combination [2]−[3] is automatically determined. For instance, if [1]−[2] and [1]−[3] show metallic and linear transport, the combination [2]−[3] will also be metallic. This because the connection point is common. However, for the "Delta" connection, the connections of the branch pairs being distinct, the combinations [1]−[2], [1]−[3], and [2]−[3] will be independent and can show different behavior. Our observation that two of the branch combinations are linear (metallic type) with no photoactivity while one branch combination shows nonlinear semiconducting-type behavior and also substantial photoactivity strongly suggests that the Y-CNT used here have "Delta" connection in the junction region. In that case we can locate the photoactivity at the point where the branches [2] and [3] make contact.

We further develop this model of the junction region based on the important observation that the photoresponse shows a zero-bias photocurrent. A zero-bias photocurrent generally arises due to photovoltaic mechanism where the electron−hole pair is separated by built-in bias from a rectifying contact. The measured $I-V$ curve though nonlinear and asymmetric does not show a strongly rectifying behavior as is expected from a single p−n junction/Schottky-type contact and observed in some Y-CNT measurements.[6] However, the observed $I-V$ curve in the present investigation can be explained if the branch connection 23 contains a back-to-back Schottky-type junction. It needs to be qualified that the Schottky-type junction can arise due to depletion layer that forms when two nanotube regions with different band gaps join. Hence, the proposed structure of the Y-CNT junction is shown in the schematic in Figure 5c. Junction of the three branches forms a "Delta" connection, of which the branch contact 23 consists of back-to-back Schottky junctions (with barriers). This arrangement results in ohmic behavior for 12 and 13 contacts and a semiconducting 23 contact.

The $I-V$ characteristics are obtained for branch combination [2]−[3] using the above model of back-to-back junctions connected by a series resistance which we mark as R_{YCNT}.[27] The current I for this MSM device can be written[28] as

$$I(V) = I_0\left[\exp\left(\frac{qV'}{\eta kT}\right) - 1\right] \times \frac{\exp\left(\frac{-q(\varphi_1+\varphi_2)}{kT}\right)}{\exp\left(\frac{-q\varphi_2}{kT}\right) + \exp\left(\frac{-q\varphi_1}{kT}\right)\exp\left(\frac{qV'}{\eta KT}\right)} \tag{1}$$

where $V' = V - IR_{YCNT}$ and I_0 arises from thermionic emission. The two Schottky-type contacts have different barrier heights φ_1, φ_2 in view of the asymmetry in the data. In such a configuration one of the junctions is always forward biased and one reversed. As a result the barrier height of the reversed bias junction controls the current flow. The fitted data with eq 1 has been shown as solid lines in Figure 2c. The barrier heights observed are ≈0.22 eV. To be exact, the best fit is obtained with φ_1 = 0.23 eV, φ_2 = 0.22 eV. The small difference shows as small asymmetry in the $I-V$ curve. These barriers are comparable to other reports on single semiconducting nanotube[29] and nanowire.[30]

The zero-bias photoresponse shows that the built-in electric field at the inner contacts collect the charge after separation. The finite current happens due to the slight difference in the barrier potentials that breaks the symmetry of the two junctions. Since the photogenerated carriers are created in the close proximity of the Schottky-type contacts, there is a possibility that the barriers heights will be lowered due to increase in carrier concentrations (n) that changes the chemical potential. The fit of the $I-V$ data under illumination is used to estimate the lowering of the barrier heights. For both the contacts, barrier heights reduces by 0.3 eV ($\Delta\varphi$) for an illumination of 21 mW at λ_1. If it is due to lowering of chemical potential due to photogenerated carriers, then ($\Delta\varphi \approx (k_BT/q)$ n_{ph}/n_0), where q is the magnitude of the electronic charge, k_B is the Boltzmann constant, n_{ph} is the carrier concentration after illumination, and n_0 is the carrier concentration in the dark. Using the above relation, we find $n_{ph}/n_0 \approx 12$. This is the order

DOI: 10.1021/acsami.6b04231
ACS Appl. Mater. Interfaces 2016, 8, 19024−19030

of the change in the carrier density that occurs in the Y-CNT branch contact region.

The presence of catalyst particle in the junction region or even due to different energy level spacings/spectrum due to different tube diameters of the branches may be responsible for such photoresponse. Since these can vary depending on the synthesis process, it is likely that the behavior that we have observed will be the same/similar to all Y-CNTs.

■ CONCLUSIONS

In summary, we report photoresponse in a single Y-CNT using pairwise branch combinations while the third branch is grounded. It is reported that the photoresponse in the given Y-CNT arises only in one branch combination ([2]−[3]) that show nonlinear and asymmetric *I*−*V* curve, while the two other branch combinations ([1]−[2] and [1]−[3]) show linear *I*−*V* curves and are photoinactive. The photoresponse observed for a single Y-CNT, in the range of 1.6 mA/W, is reasonable considering the photoresponse in single CNTs; in particular, the responsivity is higher than that reported in the bundle of SWNT and MWNTs. It must be noted that there is no published report of optical response in Y-CNT.

On the basis of the observation of a single photoactive branch combination ([2]−[3]) in the Y-CNT, a model for the connectivity of the branches in the junction region is proposed. It is also proposed that the photoresponse does not arise in the branches, but it arises in the junction region, where the combination [2]−[3] meet in a semiconductor-like junction. The photoresponse experiment thus gives us an important tool that allows us to understand the internal connectivity in a Y-CNT.

■ ASSOCIATED CONTENT

Supporting Information

The Supporting Information is available free of charge on the ACS Publications website at DOI: 10.1021/acsami.6b04231.

> Temperature (20−300 K)-dependent resistivity ρ in Y-CNT for all possible branch combinations like [1]−[2], [1]−[3], and [2]−[3], keeping one of the arms disconnected (Figure S1) (PDF)

■ AUTHOR INFORMATION

Corresponding Authors

*E-mail: sudeshna.samanta@hpstar.ac.cn. Phone: +91 033 2335 5708. Fax: +91 033 2335 3477.

*E-mail: arup@bose.res.in.

Present Address

⊥Centre for High Pressure Science & Technology Advanced Research, Shanghai, China.

Notes

The authors declare no competing financial interest.

■ ACKNOWLEDGMENTS

A.K.R. and S.S. thank Nanomission, Department of Science and Technology, Govt. of India, for financial support as a sponsored project Unit for Nanosciences. A.K.R. acknowledges additional support from the Theme Unit of Excellence in Nanodevice Technology and J.C. Bose Fellowship. A.R. and D.S. acknowledge the support provided by the American Physical Society and the Indo-US Science and Technology Forum (IUSSTF) through the India-US Physics Visitation Program.

■ REFERENCES

(1) Iijima, S. Helical Microtubules of Graphitic Carbon. *Nature* **1991**, *354*, 56−58.

(2) McEuen, P. L. Nanotechnology: Carbon-based Electronics. *Nature* **1998**, *393*, 15−17.

(3) Avouris, P.; Freitag, M.; Perebeinos, V. Carbon-Nanotube Photonics and Optoelectronics. *Nat. Photonics* **2008**, *2*, 341−350.

(4) Biercuk, M. J.; Ilani, S.; Marcus, C. M.; McEuen, P. L. Electrical Transport in Single-Walled Carbon Nanotubes. In *Carbon Nanotubes, Topics in Applied Physics*; Jrio, A., Dresselhaus, G., Dresselhaus, M. S., Eds.; Springer Verlag: Berlin, 2008; pp 455−493.

(5) Biro, L. P.; Horvath, Z. E.; Mark, G. I.; Osvath, Z.; Koos, A. A.; Benito, A. M.; Maser, W.; Lambin, Ph. Carbon Nanotube Y-Junctions: Growth and Properties. *Diamond Relat. Mater.* **2004**, *13*, 241−249.

(6) Bandaru, P. R. Electrical Characterization of Carbon Nanotube Y-Junctions: A Foundation for New Nanoelectronics. *J. Mater. Sci.* **2007**, *42*, 1809−1818.

(7) Bandaru, P. R.; Daraio, C.; Jin, S.; Rao, A. M. Novel Electrical Switching Behaviour and Logic in Carbon Nanotube Y-Junctions. *Nat. Mater.* **2005**, *4*, 663−666.

(8) Satishkumar, B. C.; Thomas, P. J.; Govindaraj, A.; Rao, C. N. R. Y-Junction Carbon Nanotubes. *Appl. Phys. Lett.* **2000**, *77*, 2530.

(9) Andriotis, A. N.; Menon, M.; Srivastava, D.; Chernozatonskii, L. Transport Properties of Single-Wall Carbon Nanotube Y-Junctions. *Phys. Rev. B: Condens. Matter Mater. Phys.* **2002**, *65*, 165416.

(10) Papadopoulos, C.; Rakitin, A.; Li, J.; Vedeneev, A. S.; Xu, J. M. Electronic Transport in Y-Junction Carbon Nanotubes. *Phys. Rev. Lett.* **2000**, *85*, 3476−3479.

(11) Dresselhaus, M. S.; Dresselhaus, G.; Saito, R.; Jorio, A. Exciton Photophysics of Carbon Nanotubes. *Annu. Rev. Phys. Chem.* **2007**, *58*, 719−747.

(12) Gabor, N. M.; Zhong, Z.; Bosnick, K.; Park, J.; McEuen, P. L. Extremely Efficient Multiple Electron-Hole Pair Generation in Carbon Nanotube Photodiodes. *Science* **2009**, *325*, 1367−1371.

(13) Shi, Y.; Fu, D.; Marsh, D. H.; Rance, G. A.; Khlobystov, A. N.; Li, L.-J. Photoresponse in Self-Assembled Films of Carbon Nanotubes. *J. Phys. Chem. C* **2008**, *112*, 13004−13009.

(14) Wei, J. Q.; Sun, J. L.; Zhu, J. L.; Wang, K. L.; Wang, Z. C.; Luo, J. B.; Wu, D. H.; Cao, A. Carbon Nanotube Macrobundles for Light Sensing. *Small* **2006**, *2*, 988−993.

(15) Lien, D.-H.; Hsu, W.-K.; Zan, H.-W.; Tai, N.-H.; Tsai, C.-H. Photocurrent Amplification at Carbon-Nanotube-Metal Contacts. *Adv. Mater.* **2006**, *18*, 98−103.

(16) Lu, S.; Panchapakesan, B. Photoconductivity in Single Wall Carbon Nanotube Sheets. *Nanotechnology* **2006**, *17*, 1843−1850.

(17) Guo, J.; Alam, M. A.; Yoon, Y. Theoretical Investigation on Photoconductivity of Single Intrinsic Carbon Nanotubes. *Appl. Phys. Lett.* **2006**, *88*, 133111.

(18) Stewart, D.; Leonard, F. Photocurrents in Nanotube Junctions. *Phys. Rev. Lett.* **2004**, *93*, 107401.

(19) Freitag, M.; Martin, Y.; Misewich, J. A.; Martel, R.; Avouris, Ph. Photoconductivity of Single Carbon Nanotubes. *Nano Lett.* **2003**, *3*, 1067−1071.

(20) Fujiwara, A.; Matsuoka, Y.; Suematsu, H.; Ogawa, N.; Miyano, K.; Kataura, H.; Maniwa, Y.; Suzuki, S.; Achiba, Y. Photoconductivity in Semiconducting Single-Walled Carbon Nanotubes. *Jpn. J. Appl. Phys.* **2001**, *40*, L1229−L1231.

(21) Barkelid, M.; Zwiller, V. Photocurrent Generation in Semiconducting and Metallic Carbon Nanotubes. *Nat. Photonics* **2013**, *8*, 47−51.

(22) Bachtold, A.; Henny, M.; Terrier, C.; Strunk, C.; Schönenberger, C.; Salvetat, J.-P.; Bonard, J.-M.; Forró, L. Contacting Carbon Nanotubes Selectively with Low-Ohmic Contacts for Four-Probe Electric Measurements. *Appl. Phys. Lett.* **1998**, *73*, 274−276.

(23) Rose, A. *Concepts in Photoconductivity and Allied Problems*; Krieger: New York, 1978. (Note: Power density of illumination corresponds to $\approx 1.3 \times 10^7$ W/m^2 for an illumination of 1 mW. If all the radiation falling on the Y-CNT is absorbed for carrier generation, an illumination of 1 mW will lead to a power absorption of $\approx$0.5 μW

over the length of the three branches. This gives an upper estimate of the power absorption.)

(24) Ahn, Y.; Dunning, J.; Park, J. Scanning Photocurrent Imaging and Electronic Band Studies in Silicon Nanowire Field Effect Transistors. *Nano Lett.* **2005**, *5* (7), 1367−1370.

(25) Basori, R.; Das, K.; Kumar, P.; Narayan, K. S.; Raychaudhuri, A. K. Single CuTCNQ Charge Transfer Complex Nanowire as Ultra High Responsivity Photo-detector. *Opt. Express* **2014**, *22*, 4944−4952.

(26) Rabbani, M. G.; Patil, S. R.; Verma, A.; Villarreal, J. E.; Korgel, B. A.; Nekovei, R.; Khader, M. M.; Darling, R. B.; Anantram, M. P. Zero-Bias Photocurrents in Highly-Disordered Networks of Ge and Si Nanowires. *Nanotechnology* **2016**, *27*, 045201.

(27) Samanta, S.; Das, K.; Raychaudhuri, A. K. Junction Effect on Transport Properties of a Single SiNanowire Metal-Semiconductor-Metal Device. *IEEE Trans. Nanotechnol.* **2013**, *12*, 1089−1094.

(28) Norde, H. A. Modified Forward I-V Plot for Schottky Diodes with High Series Resistance. *J. Appl. Phys.* **1979**, *50*, 5052−5053.

(29) Behnam, A.; Johnson, J. L.; Choi, Y.; Ertosun, M. G.; Okyay, A. K.; Kapur, P.; Saraswat, K. C.; Ural, A. Experimental Characterization of Single-Walled Carbon Nanotube Film-Si Schottky Contacts Using Metal-Semiconductor-Metal Structures. *Appl. Phys. Lett.* **2008**, *92*, 243116.

(30) Samanta, S.; Das, K.; Raychaudhuri, A. K. Low-Frequency Flicker Noise in a MSM Device Made with Single Si Nanowire (diameter ≈ 50 nm). *Nanoscale Res. Lett.* **2013**, *8*, 165.

DOI: 10.1021/acsami.6b04231
ACS Appl. Mater. Interfaces 2016, 8, 19024−19030